Instantaneous Time-Courses of Baroreflex Sensitivity, Sympathetic and Vagal Activities in Response to Mueller Maneuver

Salvador Carrasco-Sosa, Alejandra Guillén-Mandujano

Universidad Autónoma Metropolitana-Iztapalapa, CDMX, México

Abstract

We assessed, in 37 recordings of healthy volunteers, the effects induced by Mueller maneuver (MM) on the time-courses of the high frequency component of RR (HF_{RR}), the low frequency components of RR (LF_{RR}), systolic (LF_{SBP}) and diastolic blood pressure (LF_{DBP}), estimated by a time frequency distribution, and baroreflex sensitivity (BRS) computed by alpha index. Ensemble averages of indexes dynamics showed: SBP and DBP, after a fall in early strain (S_E), increased gradually in late strain (S_L), peaking in early post-strain (PS_E). Similarly, LF_{RR}, LF_{SBP} and LF_{DBP} raised, but peaked in S_L, heart rate (HR) and LF_{RR}/HF_{RR} remained elevated through S_E, S_L and PS_E. All recovered gradually and fell below their baseline in late post strain (PS_L). BRS and HF_{RR} decreased during S_E and S_L and increased in PS_L. In S_L and PS_L, LF_{SBP}-SBP and LF_{DBP}-DBP correlations ranged from 0.60 to 0.83. MM induces, in S_L and PS_E, via the interaction of chemoreflex and baroreflex with reduced BRS, increments of sympathetic outflow and vagal withdrawal, effects associated to rising SBP, DBP, and HR; and, in PS_L, via baroreflex, now with augmented gain, evokes gradual reduction of sympathetic activity and increment of vagal outflow, leading to cardiodecelerative and hypotensive effects. This functional picture suggests that BRS changes possibly contribute to driving the autonomic cardiovascular response to MM.

1. Introduction

Mueller maneuver (MM), the opposite respiratory strain of Valsalva maneuver, has been used: as a physiological model that consistently mimics the sympathetic pressor effects of obstructive sleep apnea (OSA) [1, 2]; as a therapeutic procedure for cardiovascular diseases that course with central hypovolemia, because loaded inspiration leading to an intrathoracic pressure of around -10 cmH_2O increases perfusion to organs such as the brain and the heart [3]; by physicians, to accentuate right heart sounds and to improve the contrast density of pulmonary vasculature in computerized tomographic imaging [4].

Despite its clinical and physiological relevance, the autonomic-cardiovascular response evoked by MM has not been as extensively studied as that of its counterpart Valsalva maneuver, and its underlying functional mechanisms have not been sufficiently clarified, probably due in part to the contradictory findings reported [5]. There is not an agreement on the autonomic-cardiovascular effects that MM induces, nor detailed and comprehensive revisions that study them.

A relevant characteristic of baroreflex sensitivity (BRS) when computed by the modern spectral methods is that it provides more functional information by enabling the tracking of its instantaneous time-course through the experimental conditions, while the pharmacological and neck chamber methods only provide punctual BRS values. Thus, for example, using time-varying methods, it was possible to document the gradual decrease in BRS in the head-up tilt test [6].

Considering the reported evidence that muscular sympathetic nerve activity (MSNA) increases in MM strain (S) and decreases in its post-strain (PS) [2, 5, 7], and that in OSA BRS decreases and the low-to-high frequency ratio of RR intervals (LF_{RR}/HF_{RR}) increases, associated with the pressor effect [1], we hypothesize that, in MM S, BRS will decrease, associated with the elevation of the low frequency power of systolic blood pressure (LF_{SBP}) and of LF_{RR}/HF_{RR}, and that, in the PS, these indexes will present the opposite changes. Thus, we assessed, in 37 recordings of healthy volunteers, the effects provoked by MM on the time-courses of R-R intervals (RR), systolic (SBP), diastolic (DBP) and pulse pressures (PP), from which we estimated, using a time-frequency distribution, the dynamics of low frequency components of RR (LF_{RR}), LF_{SBP} and DBP (LF_{DBP}); high frequency power of RR (HF_{RR}), BRS by α-index, and its coherence (BRS_{CO}).

2. Methods

2.1. Subjects

Thirty (18 male and 12 female), young, healthy, non-smoking, non-addicted, and sedentary subjects participated. Age, weight, and height were 23.2±2.4 years, 64.4±10.3 kg and 165±10 cm respectively. Their written

informed consent was requested to participate.

2.2. Protocol

Volunteers visited the laboratory twice. In the first visit, their health status was evaluated, and they were trained to perform MM correctly. In the second visit, the experimental condition was carried out, which comprised three successive stages: control, 1 min long, maneuver, 20 s long, and recovery, 2 min long. Subjects performed MM twice, in sitting position and aided by visual feedback that displayed the mouth pressure (MP) level. 10 s before the maneuver execution, subjects were notified. MM strain was achieved by performing an inspiratory effort into a closed tube to sustain a MP of -40 mmHg for 20 s, with a 5-min rest period between tests.

2.3. Signal recording and acquisition

ECG was detected at CM5 lead using a bioelectric amplifier (Biopac Systems). Noninvasive arterial pressure was recorded by Finapres (Ohmeda). Respiratory movements were measured by a pneumograph (Biopac Systems). MP was recorded by a pressure transducer (Validyne) connected to the distal end of a closed tube which had a mouthpiece attached to the proximal end. All signals were digitized at a sampling rate of 1 kHz via an acquisition and display system (Biopac Systems).

2.4. Data processing

From 37 valid recordings, R-wave peaks of ECG and fiducial points of arterial pressure signals were beat-to-beat detected to generate the time series of RR, SBP, DBP, and PP (as SBP-DBP difference). These were cubic-spline interpolated, resampled at 4 Hz and detrended by the smoothness priors method. Auto- and cross time-frequency spectra of RR, SBP and DBP were estimated with the smoothed pseudo-Wigner-Villé TFD. We extracted the instantaneous HF_{RR}, LF_{RR}, LF_{SBP}, LF_{DBP} from the first moment of their TFD in the standard HRV low- and high-frequency bands, from which we computed: the LF_{RR}/HF_{RR} ratio, BRS by α-index ($\sqrt{LF_{RR}/LF_{SBP}}$), and the respective BRS_{CO} by cross-time-frequency analysis. To better depicting the changes of the dynamics of the indexes used, the S and PS phases of MM were divided, based on the inflection points shown by SBP dynamics, into: early S (S_E), from the initial fall to the minimum SBP; late S (S_L), from the previous limiting point (LP) to the final rise; early PS (PS_E), up the maximum SBP; and late PS (PS_L) as the remaining period. The LP were detected semi-automatically on each recording of SBP. To highlight any patterned responses to MM, individual indexes dynamics were ensemble-averaged once their mean baseline (BL) level was subtracted.

2.5. Statistical analysis

Data were expressed as mean ± SD. Differences among the LP of each index dynamics, including mean BL, were tested by ANOVA for repeated measures, with post-hoc pairwise comparisons by the Tukey test. Pairs of linear regressions and correlations of LF_{SBP} with SBP and of LF_{DBP} with DBP were computed using the data segments of S_L and PS_L. Statistical significance was set at $p<0.05$.

3. Results

In general, the LP means were different from their mean BL ($p<0.03$). Mean values of the autonomic cardiovascular variables (ACVV) dynamics in the 10 s prior to the beginning of MM S (anticipatory phase, AP), raised significantly ($p<0.01$), except BRS dynamics, which decreased ($p<0.01$). In general, these changes were attenuated by the onset of MM S (Fig. 1 and 2).

The changes in the ensemble averages of the ACVV dynamics through the phases of MM were: SBP (Fig. 1A) presented an initial drop that persisted during S_E, a gradual rise in S_L that reached its maximum in PS_E, followed by a gradual recovery and decline below BL in PS_L (-5.6±12.5 mmHg, $p<0.01$). DBP and PP dynamics (Fig. 1B and C) showed changes similar to those of SBP but of smaller amplitude. DBP showed a mean decrease of -7.7±6.3 mmHg in the PS_L phase (Fig. 1B), while PP remained elevated (Fig. 1C). Heart rate (HR) increased during S and decreased below BL at PS_E, level that was maintained for the rest of the recording (Fig. 1D).

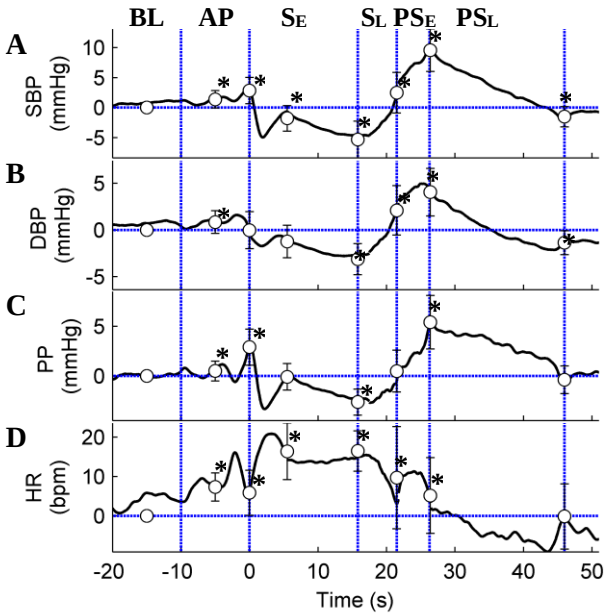

Fig. 1. Ensemble averages and LP means±SD of the time courses of: A) SBP, B) DBP, C) PP and D) HR. *$p<0.001$ vs. mean BL.

BRS (Fig. 2A) decreased in S_E phase to rise progressively, surpassing its BL level in PS_E and reaching a maximum at 30 s of the PS_L phase. BRS_{CO} (Fig. 2B) remained above 0.71 in the AP and during S and PS. LF_{RR} (Fig. 2F), LF_{SBP} (Fig. 2C) and LF_{DBP} (Fig. 2D) dynamics showed similar changes: after an initial decline that lasted until S_E (the one of LF_{RR} below BL) they showed a progressive increase to reach a maximum at S_L, and then gradually recover towards BL, with the difference that LF_{SBP} and LF_{DBP} fell below their BL ($p<0.01$). HF_{RR} (Fig. 2E), after an initial decline, gradually increased, surpassing its BL at S_L, peaked at PS_L, and declined slightly, though it remained above BL for the rest of the record.

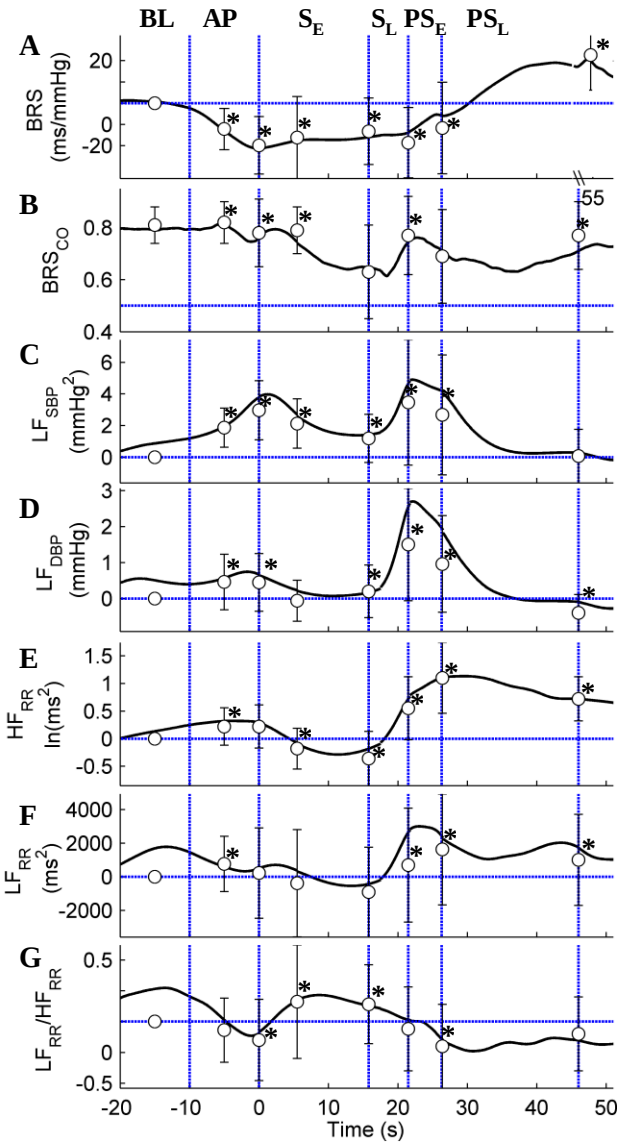

Fig. 2. Ensemble averages and LP means±SD of the time courses of: A) BRS, B) BRS_{CO}, C) LF_{SBP}, D) LF_{DBP}, E) HF_{RR}, F) LF_{RR}, G) LF_{RR}/HF_{RR} spectral measures. *p<0.001 vs. mean BL.

The LF_{RR}/HF_{RR} ratio (Fig. 2G) increased at the beginning of S_E, gradually decreased in S_L to below the BL in PS_E and persisted reduced in PS_L.

LF_{SBP}-SBP and LF_{DBP}-DBP relations showed significant correlations ($p<0.001$) in S_L phase ($r_{LFSBP\text{-}SBP}$= 0.83±0.16, $r_{LFDBP\text{-}DBP}$= 0.78±0.22) and in PS_L phase ($r_{LFSBP\text{-}SBP}$=0.65±0.38, $r_{LFDBP\text{-}DBP}$=0.60±0.42) (Fig. 3).

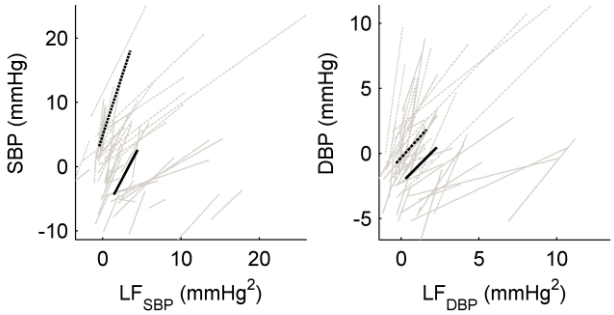

Fig. 3. Individual (grey) and mean (black) linear regressions in S (solid) and PS (dashed) of LF_{SBP}-SBP and LF_{DBP}-DBP relationships.

4. Discussion

Our approach, based on the computing of the instantaneous time-courses of the noninvasive, reliable indexes of cardiac -LF_{RR}- and vasomotor -LF_{SBP}- sympathetic activity, vagal -HF_{RR}- [8] and BRS (obtained by alpha index, $\sqrt{LF_{RR}/LF_{SBP}}$) [6], allowed us to organize them in a plausible time sequence with a cause-effect format, explanatory of the ACVV response to MM.

It has been well documented that the increase in blood pressure during S_L and PS_E of MM is caused by increased sympathetic vasomotor activity, a notion supported by the parallel increases in MSNA (preceded by its decrease), and in blood pressure [2, 5, 7], and by the abolition of this effect achieved by ganglionic blockade with trimethaphan [5]. The sympathetic spectral indicators that we used correctly indicated the initial decrease of MSNA followed by its increase (Fig. 2 C, D, F) and the associated elevations in SBP and DBP (Fig. 1 A, B), relationship also supported by the strong correlations obtained between them in S and PS (Fig. 3). Furthermore, HF_{RR} changes evidenced vagal withdrawal during S and vagal increase in PS (Fig. 2E).

The increase in sympathetic activity in MM has been attributed to the activation of the chemoreflex (ChR), triggered by the hypercapnia-hypoxia caused by 20-s voluntary apnea, notion supported by the suppression of the pressor sympathetic response by the previous administration of supplemental O_2 [7]. The increment in HR [5, 7] and the mechanical effects of negative intrathoracic pressure on cardiovascular function would play a minor role, because they only evoke a decrease in stroke volume due to a reduction in preload and an increase in afterload during S [5, 7], which increase during PS. However, our findings suggest that, in addition to the ChR,

there is a relevant participation of: central command (CC) for the global performance of MM; arterial baroreflex (BR) that contributes to the generation of the pressor response and its recovery in PS, cardiac output (CO) increased by rises in HR and stroke volume, indicated by the dynamics of PP, and cardiopulmonary baroreflex (CPBR), involved in the sympathetic inhibition in S_E. The timing of the changes between the autonomic and cardiovascular indices and the high correlations between them that we found (Fig. 3), allow us to make some sequential cause-effect considerations. Thus, the decrease in blood pressure and BRS (Fig. 2A) during S_E precedes the gradual increase in LF_{RR} (Fig. 2F), LF_{SBP} (Fig. 2C) and LF_{DBP} (Fig 2D), associated with increases in SBP (Fig 1A) and DBP (Fig 1B), changes that again precede the increase in BRS (Fig. 2A) and the gradual decrease of sympathetic indices and increase in the vagal index (Fig. 2E) in PS_L, associated with a decrease in SBP and DBP and an increase in HR (Fig. 1D). This sequence supports our explanatory functional mechanism: the CC, in a visually guided manner, anticipates, initiates, maintains, and terminates the activity of the respiratory muscles that perform the inspiratory effort that causes the sustained decrease in intrathoracic pressure and the associated apnea, and, in parallel, makes the corresponding autonomic-cardiovascular adjustments. In the AP, CC induces a decrease in BRS and an increase in cardiac sympathetic and vasomotor activity (Fig. 2), associated with slight increases in blood pressure and HR (Fig. 1). The beginning of S_E provokes a sudden drop in arterial pressure and an increase in venous return that, by raising the right atrium pressure, loads the cardiopulmonary baroreceptors, which, by inducing sympathetic inhibition, accentuate the drop in blood pressure (Fig. 1 and 2). This stimulus, via the BR with decreased sensitivity (Fig. 2A), together with the relevant contribution of the ChR, induces an increase in vasomotor (Fig. 2C and D) and cardiac (Fig. 2F) sympathetic activity and vagal withdrawal (Fig. 2E), which cause, through gradual increases in peripheral vascular resistance (PVR) and CO in S_L that progressively increases SBP (Fig. 1A), DBP (Fig. 1B) and PP (Fig. 1C). At the end of S_L, thoracic and cardiovascular retraction, together with the persistent increases in CO and PVR, cause a further increase in SBP and DBP, which peak in PS_E. This stimulus, via the BR with slightly decreased sensitivity (Fig. 2A), decreases cardiac (Fig. 2F) and vasomotor (Fig. 2C and D) sympathetic activity, and increases vagal activity (Fig. 2E), autonomic effects associated with the increase in BRS (Fig. 2A) and the gradual recovery of SBP and DBP towards BL, which becomes hypotension with cardiodeceleration (Fig. 1). The association between the decrease in BRS and the predominance of sympathetic activity, indicated by the LF_{RR}/HF_{RR}, in S, and the increase in BRS associated with the predominance of vagal activity in PS (Fig. 2G), suggest that changes in BRS possibly manage the sympathovagal balance response to MM.

In conclusion, the cardiovascular response to MM results from the interplay of mechanical and autonomic effects, driven by the interaction of the CC, ChR, BR, and CPBR. Thus, the ChR and BR with reduced sensitivity induce increments of cardiac and vasomotor sympathetic outflow and reduction of vagal activity in the S_L stage, provoking the rise of SBP, DBP, and cardioacceleration, and, in the PS_E, greater elevations of SBP and DBP that, via BR, now with augmented gain, cause gradual reduction of cardiac and vasomotor sympathetic activities and increment of vagal outflow, leading to cardiodeceleration and hypotension in PS_L. This functional picture suggests that BRS adjustments possibly contribute to driving the autonomic cardiovascular response to MM.

References

[1] Lombardi C, Pengo MF, Parati G. Obstructive sleep apnea syndrome and autonomic dysfunction. Auton Neurosci. 2019;221:102563. doi:10.1016/j.autneu.2019.102563

[2] Taylor KS, Keir DA, Haruki N, et al. Comparison of Cortical Autonomic Network-Linked Sympathetic Excitation by Mueller Maneuvers and Breath-Holds in Subjects With and Without Obstructive Sleep Apnea. Front Physiol. 2021;12:678630. Published 2021 May 26. doi:10.3389/fphys.2021.678630

[3] Convertino VA. Mechanisms of inspiration that modulate cardiovascular control: the other side of breathing. J Appl Physiol. 2019;127(5):1187-1196

[4] Gutzeit A, Froehlich JM, Wälti S, et al. Suction/Inspiration against resistance or standardized Mueller maneuver : a new breathing technique to improve contrast density within the pulmonary artery: a pilot CT study. Eur Radiol. 2015;25(11):3133-3142.

[5] Katragadda S, Xie A, Puleo D, et al. Neural mechanism of the pressor response to obstructive and nonobstructive apnea. J Appl Physiol. 1997;83(6):2048-2054.

[6] Orini M, Laguna P, Mainardi LT, Bailón R. Assessment of the dynamic interactions between heart rate and arterial pressure by the cross time-frequency analysis. Physiol Meas. 2012;33(3):315-331.

[7] Morgan BJ, Denahan T, Ebert TJ. Neurocirculatory consequences of negative intrathoracic pressure vs. asphyxia during voluntary apnea. J Appl Physiol. 1993;74(6):2969-2975.

[8] Schnekenberg L, Sedghi A, Schoene D, et al. Assessment and Therapeutic Modulation of Heart Rate Variability: Potential Implications in Patients with COVID-19. J Cardiovasc Dev Dis. 2023;10(7):297. Published 2023 Jul 12. doi:10.3390/jcdd10070297

Address for correspondence:

Salvador Carrasco-Sosa
Depto. Ciencias de la Salud, UAM-I
Av. San Rafael Atlixco # 186, C.P. 09340 Cd. Mx., México.
scas@xanum.uam.mx